Improved Hydrogen Storage and Thermal Conductivity in High-Density MOF-5 Composites

Justin Purewal,*,†,# Dongan Liu,†,§ Andrea Sudik,‡,∥ Mike Veenstra,‡ Jun Yang,‡ Stefan Maurer,¶ Ulrich Müller,¶ and Donald J. Siegel*,†

†Mechanical Engineering Department, University of Michigan, 2350 Hayward Street, Ann Arbor, Michigan 48109, United States
‡Ford Motor Company, Research and Advanced Engineering, MD 1170/RIC, Dearborn, Michigan 48121, United States
¶BASF SE, Chemicals Research and Engineering, 67056 Ludwigshafen, Germany

ⓢ Supporting Information

ABSTRACT: Porous adsorbents such as MOF-5 have low thermal conductivities which can limit the performance of adsorption-based hydrogen storage systems. To improve the thermal properties of these materials, we have prepared a series of high-density MOF-5 composites containing 0−10 wt % expanded natural graphite (ENG), which serves as a thermal conduction enhancer. The addition of 10 wt % ENG to MOF-5 and compaction to 0.5 g/cm^3 was previously found to increase the thermal conductivity relative to neat MOF-5 of the same density by a factor of 5. In this study, detailed measurements of the hydrogen storage behavior of MOF-5/ENG composites between 77 and 295 K are reported. We find that MOF-5 pellets with 0 wt % ENG and a density of 0.5 g/cm^3 have a total volumetric hydrogen storage density at 77 K and 100 bar that is 23% larger than powder MOF-5 and 41% larger than cryo-compressed hydrogen. The addition of 10% ENG to 0.5 g/cm^3

MOF-5 pellets produces only a small decrease (6%) in the total volumetric hydrogen storage compared to neat MOF-5 pellets of equal density. The excess, absolute, total, and deliverable hydrogen storage amounts by the MOF-5 composites are compared for ENG additions of 0−10 wt % and pellet densities of 0.3−0.7 g/cm^3. Three adsorption models (Unilan, Tóth, Dubinin−Astakhov) are compared for their effectiveness in describing hydrogen adsorption isotherms of MOF-5 and MOF-5/ENG composites. The Unilan model provides the most accurate description of the experimental data, requiring only five temperature-invariant parameters to accurately fit the data across a wide temperature range.
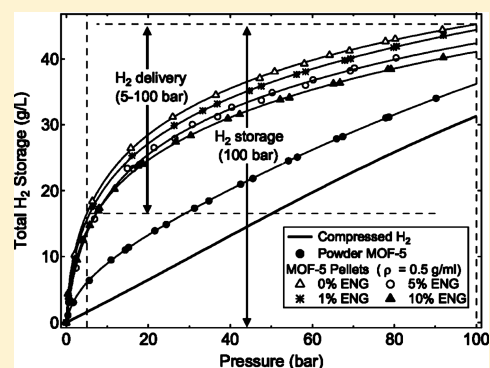
INTRODUCTION

While materials discovery has been a focus of most hydrogen storage research, the integration of a given storage material into a viable storage system remains an equally important problem.[1] Engineering challenges include optimizing the following: (a) packing density, (b) heat and mass transfer, and (c) hydrogen uptake properties of adsorbent materials. In this study we have used metal−organic framework MOF-5 as a prototype material for exploring processing strategies that maximize heat transfer and packing density while preserving hydrogen storage capacity. MOF-5 consists of ZnO_4 clusters connected by 1,4-benzenedicarboxylate (BDC) linkers.[2] This compound is one of the most thoroughly studied adsorbent materials, and large numbers of H_2 adsorption measurements have been published. Depending on synthesis, postprocessing, and activation methods, the maximum excess hydrogen adsorption at 77 K for MOF-5 has been measured at 4.3,[3] 4.9,[4] 5.1,[5] 5.8,[6,7] and 7.1 wt %.[8] The isosteric heat has been estimated at 3.8,[5] 4.0,[9] 4.1,[3] 4.8,[7] and 4.7−5.2 kJ/mol.[10]

Although characterization of the excess adsorption by MOF-5 is important, it is the *total* storage capacity that is most relevant from a systems perspective. The total capacity includes both the excess hydrogen near the adsorbent surface plus the bulk hydrogen gas residing throughout the entire void volume (intracrystalline pores, intercrystalline voids, interstitial spaces). Since MOF-5 is commonly synthesized as a powder (crystallite size less than 1 μm) with low bulk density (0.13−0.2 g/cm^3), it is advantageous to process the powder into pellets or extrudates which minimize the presence of interstitial spaces, where the amount of higher-density adsorbed hydrogen will be small.[11−13] Compacted pellets, rather than loose powders, are more attractive for on-board gas storage applications due to the potentially larger volumetric storage density and the improved ease of handling. In a previous study we found that MOF-5 compaction produced modest decreases in the gravimetric hydrogen storage capacity, offset by much larger increases in the volumetric capacity.[14] Micropore volume decreased with compaction due to amorphization of the MOF-5 crystal structure;[15] however, it was possible to mitigate this effect by controlling the pellet density. Similar results for the compaction

of MOF-177[16,17] and activated carbons[18] have also been reported.

Due to their large pore sizes (e.g., >20 Å diameter) and high free volumes (e.g., >90%), the thermal conductivity of many microporous materials (e.g., zeolites, MOFs) is unusually low. This low conductivity can place limitations on the design of cryo-adsorption-based storage systems. For example, it can hinder fast refueling due to the longer cool-down times required to reach operating temperatures. Heat sources during refueling, including the released heat of adsorption, the compression work, and the thermal mass from the inlet hydrogen gas, must also be dissipated to prevent a temperature increase in the storage material.[19] Although the heat dissipation problem for cryo-sorption is not as demanding as for hydride beds, the unusually low heat conduction properties of MOFs present a significant materials engineering challenge. As an example, a vehicle-scale tank filled with 5.4 kg of Cu-BTC at 77 K that is charged with 200 bar of H_2 gas (at room temperature) over 5 min can produce an average temperature increase of 15 K near the tank center, even with the tank immersed in an LN_2 bath.[20] Extensive experimental data is also available for activated carbon sorbent beds.[21−23]

In a prior study, we reported that low-density (0.3 g/cm^3) MOF-5 pellets had a thermal conductivity below 0.1 W/mK at room temperature, slightly lower than the value of 0.3 W/mK measured for a single crystal of MOF-5.[24] To improve thermal conduction, we synthesized MOF-5-based composites containing 0−10% expanded natural graphite (ENG), with pellet densities of 0.3, 0.5, or 0.7 g/cm^3.[25] ENG (i.e., natural graphite which has been soaked in sulfuric acid and purified by heating to high temperatures) has been successfully used as a thermal conduction enhancer in a variety of metal and complex hydride materials.[26−28] We found that for pellets with density 0.5 g/cm^3, the addition of 10% ENG produced a factor of 5 improvement in thermal conductivity relative to neat MOF-5 pellets of equal density. Although alternate strategies for enhancing thermal conduction exist, such as packing MOF-5 powder within open-cell metal foams, composite formation may impose a smaller penalty on both volumetric and gravimetric hydrogen storage density and may be therefore better suited for the moderate heat dissipation requirements of cryo-adsorption.

As our previous study focused on the thermal properties of MOF-5/ENG composites, in the present study we explore the hydrogen storage properties of these composites at temperatures between 77 and 295 K. We compare the effectiveness of a pore-filling model (Dubinin−Astakhov) and two monolayer-based models (Unilan, Tóth) for describing MOF-5 hydrogen adsorption isotherms, comparing to both published data (30−300 K, 0−60 bar) and our own experimental measurements (77 −295 K, 0−100 bar). The Unilan model is found to produce the most accurate fits to the MOF-5 isotherms across the complete range of temperature, even while requiring only five temperature-invariant parameters. Second, the effect of varying ENG content and pellet density on the excess and total hydrogen storage properties of the MOF-5 composites is systematically investigated. Compacting powder MOF-5 to a density of 0.5 g/cm^3 is found to increase the maximum excess hydrogen adsorption at 77 K, on a volumetric basis, by a factor of about three. Adding 10 wt % ENG to the 0.5 g/cm^3 neat MOF-5 pellets for improved thermal conduction reduces the excess adsorption (volumetric and gravimetric) by approximately 12% compared to the neat pellets. Additions of 5 wt %

ENG result in less pronounced reductions in the hydrogen storage amounts, but at the expense of smaller improvements in the thermal conductivity. These results indicate that the addition of small of amounts of ENG to compacted MOF-5 provides a simple way to enhance thermal properties with only modest decreases in the hydrogen storage amounts.

■ EXPERIMENTAL DETAILS

Experimental Methods. Details on the synthesis and characterization of the as-received MOF-5 powder are available,[11,12] and our methods for preparing MOF-5/ENG composite pellets have been described previously.[14,25] The ENG composition is given as a percentage of the total pellet mass. Hydrogen adsorption was measured on a volumetric Sievert's-type instrument (PCT-Pro 2000, Setaram), with an oil-free scroll vacuum pump (Anest Iwata model ISP90). Samples masses varied between 320 and 484 mg. Prior to measurement, the samples were outgassed at 403 K under continuous vacuum for at least 6 h (3 h at room temperature, followed by 3 h at 403 K). The void volume of the sample holder was determined by helium expansion for each sample. To correct for the difference between sample temperature and the instrument temperature, the void volume was divided into a subvolume at sample temperature and a subvolume at room temperature using a fixed dividing line, with the hydrogen density evaluated separately for each subvolume.[29] To improve accuracy, we performed a calibration test for each MOF-5/ENG sample using an equivalent displacement volume of nonporous Al_2O_3 powder and identical measurement settings. Maximum adsorption during calibration tests (i.e., instrument error) was about 0.3 mmol of hydrogen, in comparison to the 10 mmol of H_2 that was typically adsorbed for each sample. Calibration curves were subtracted from the corresponding sample data, although this had only a minor effect on the results. Adsorption kinetics were rapid for the MOF-5 composites at all temperatures, even for the high-density pellets, and equilibrium was reached within 3 min. The total measurement time for adsorption and desorption cycles was fixed at 5 min for each point.

Isotherms were measured for temperatures between 77 and 295 K. The 77 K isotherms were measured using a liquid nitrogen bath; 200 K isotherms were measured with the sample holder covered in solid CO_2 powder; 295 K isotherms were measured at ambient temperature. Intermediate temperature isotherms were measured using a continuous-flow, sample-in-vapor liquid nitrogen cryostat (CryoPro-2009, Setaram). The temperature stability was within 1 K over the course of a single measurement, and the sample temperature was accurately measured using an internal platinum resistance thermometer in direct contact with the sample. The hydrogen gas density was calculated from an equation of state[29] for normal hydrogen implemented in the NIST Standard Reference Database 23.[31]

Definitions of Adsorbent Density. For porous materials there exist several definitions of density.[32] The skeletal density (ρ_{sk}), which excludes the volume of open pores, is typically measured for each sample using helium. For powder MOF-5, a value of ρ_{sk} = 2.03 g/cm^3 was determined by a helium pycnometer (AccuPyc 1339, Micromeritics). For other samples, the skeletal densities were estimated using the volumetric PCT instrument. The single-crystal density (ρ_{sc}), which includes the volume of all intracrystalline pores, is assumed to equal the theoretical MOF-5 crystallographic density (0.605 g/cm^3). The envelope density (ρ_{env}) is defined in terms of the volume within

20200

dx.doi.org/10.1021/jp305524f | *J. Phys. Chem. C* 2012, 116, 20199−20212

a close-fitting envelope enclosing a pellet and is calculated from the physical dimensions of a single pellet. The envelope density is used only for pellets, not for powder MOF-5 (for which the bulk density is used instead). The bulk density (ρ_{bulk}) includes the total volume, including all internal pore and interparticle void space, after the powder has settled following tapping or vibration. We measured the powdered MOF-5 bulk density as $\rho_{bulk} = 0.13$ g/cm^3 using a calibrated volume and approximately 10 s of tapping. We use this value for all calculations in the article, as it accurately reflects the bulk density of powder that was loaded in the Sievert's sample holder for volumetric measurements. In practice, however, the bulk density of powder MOF-5 can depend on factors such as particle size, electrostatic interactions between particles, and the method of density measurement — we found that it could vary between 0.13 and 0.2 g/cm^3.

To provide a realistic estimate of the density of an actual sorbent bed, the bulk density is used for powder MOF-5 while the envelope density is used to describe compacted MOF-5/ENG monoliths. These assumptions are consistent with the use of a compacted MOF-5 monolith within the tank. Accordingly, the specific void volume for pellets is defined as

$$v_v(\text{pellet}) = 1/\rho_{env} - 1/\rho_{sk} \tag{1}$$

while for the MOF-5 powder it is defined as

$$v_v(\text{powder}) = 1/\rho_{bulk} - 1/\rho_{sk} \tag{2}$$

The bulk density of MOF-5/ENG pellets is based on the volume of a rigid storage tank occupied by a random packing of cylindrically shaped pellets, which would be lower than the envelope density as defined above. As an estimate, the packing ratio of single-size solid spheres after settling is typically close to 60%,[33] although the packing ratio for cylindrical pellets could be improved by stacking them in close-packed arrays.

Definitions of Hydrogen Storage Density. Three definitions of adsorptive hydrogen storage density are used in this study. *Excess* adsorption (n_{ex}), as directly measured by the volumetric method, is presented here either in units of moles of H$_2$ per kilogram of adsorbent (mol/kg) or as a percentage of the combined H$_2$ and sorbent mass (wt %). *Absolute* adsorption (n_a) is related to excess adsorption by $n_a = n_{ex} + v_a\rho_g$, where v_a is the adsorbate volume and ρ_g is the bulk hydrogen gas density. The adsorbate volume is not well-defined but should enclose the regions around the adsorbent surface where local adsorptive density exceeds the bulk gas density. It may also be interpreted as the volume near the surface that is subjected to the potential field of the solid. We assume that v_a is constant with respect to adsorption amount and temperature and that $\rho_a = n_a/v_a$ equals an average adsorbate density. The magnitude of v_a should be close to the MOF-5 intracrystalline open pore volume, $v_{pore} = 1/\rho_{sc} - 1/\rho_{sk} = 1.2$ g/cm^3).

Total storage is a third measure of adsorptive hydrogen storage density. It counts the total hydrogen amount (both adsorbed and gaseous) present within the void volumes of MOF-5 pellets and powder and is important for determining the actual hydrogen delivery from a storage tank. Therefore, it provides a measure of the effectiveness of an adsorbent in increasing the storage capacity of a fixed volume when filled with the adsorbent. The total hydrogen storage amount for sorbent mass $m_{sorbent}$ is equal to $N_t = m_{sorbent}(n_{ex} + v_v\rho_g)$, where the void volume has been defined for powders (eq 2) and

pellets (eq 1). When presented as a fraction of total adsorbent volume (assuming a monolith), it has the form

$$n_{t,vol} = \rho_{env}n_{ex} + \left(1 - \frac{\rho_{env}}{\rho_{sk}}\right)\rho_g \tag{3}$$

where ρ_{env} should be replaced with ρ_{bulk} for powder MOF-5. This total volumetric storage quantity can be considered as a material property (as opposed to a system property), although it does depend on material postprocessing such as mechanical compaction and composite formation. The total gravimetric hydrogen storage is not discussed in this article.[34]
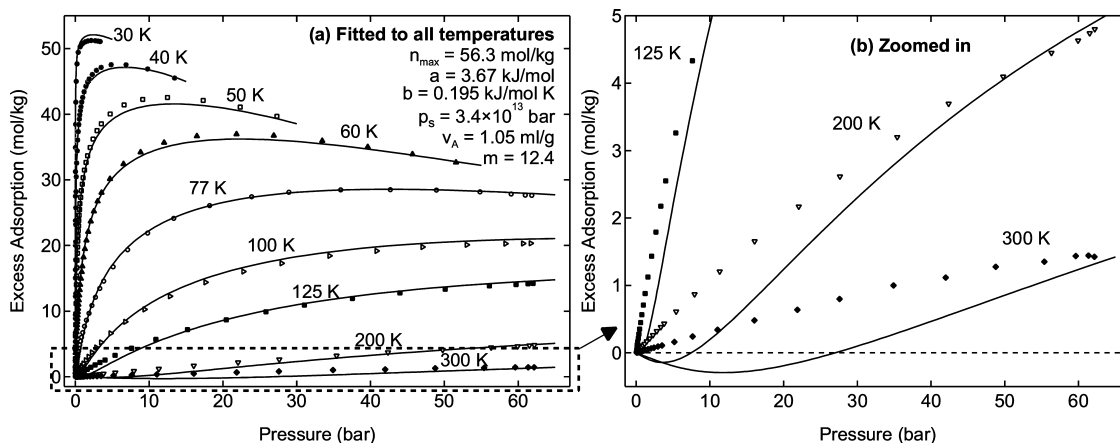
■ MODELS

Modified D–A Model. To develop realistic heat and mass balance equations for an adsorbent-based storage system, it is useful to have a model that describes the adsorption across a wide range of practical temperatures and pressures. It is also desirable to accurately determine parameters for such a model by fitting to a small number of isotherms at easily measured temperatures such as 77, 87 (liquid Ar), 200 (solid CO$_2$), and 295 K. The Dubinin–Astakhov (D–A) model[35] has been frequently used in a modified form to describe supercritical hydrogen adsorption in activated carbons,[36,37] zeolites,[38] and in the framework material Cu-BTC[21] at pressures up to 200 bar. Conceptually, the D–A model considers the adsorbed species within the micropores as similar to a liquid, although with properties that differ from the bulk liquid due to the presence of the adsorbent force field.[39] When the D–A model is modified to address excess adsorption within a constant adsorbate volume,[37] the resulting equation is given by

$$n_{ex} = n_{max}\exp\left[-\left(\frac{RT}{a+bT}\right)^m \ln^m\left(\frac{p_s}{p}\right)\right] - \rho_g v_a \tag{4}$$

where $E = a + bT$ is the characteristic energy of adsorption (i.e., assumed here to vary linearly with temperature), p_s is a pseudosaturation pressure, and m can be interpreted as a micropore heterogeneity parameter. A value of $m = 2$ appears adequate to describe hydrogen adsorption on the activated carbons AX-21 and CNS-201 and the framework material Cu-BTC.[22] For subcritical adsorption, the adsorption potential $A = -RT\ln(p/p_s)$ is considered as the difference in free energy between the adsorbate phase and the saturated liquid at the same temperature, while at supercritical temperatures a pseudosaturation pressure is substituted for p_s. The characteristic free energy E is generally temperature-invariant in the absence of electrostatic adsorbent–adsorbate interactions.[35] For a nonpolar adsorbate such as H$_2$, however, small temperature variations in E can be explained as the entropic contribution to the free energy. The linear variation $E = a + bT$ assumed in eq 4 has been found to work well empirically for hydrogen adsorption in activated carbons.[37] An inherent weakness of the D–A model is that it does not reduce to Henry's law in the low-concentration limit. Further, the absolute differential enthalpy of adsorption derived from eq 4 using the Clausius–Clapeyron equation has a logarithmic singularity at $n_a = 0$.

Although the modified D–A model has been found to work well for activated carbons such as AX-21 over a wide temperature range, our data suggest (see below) that it is less useful for describing hydrogen adsorption in crystalline porous materials such as MOF-5 which lack strong adsorption sites.

Figure 1. Fits of the modified D−A equation (eq 4) to experimental MOF-5 isotherms from ref 7. (a) Model fitted to all temperatures without constraints on m. (b) Same fits, zoomed in to the excess adsorption range of 0−5 mol/kg.
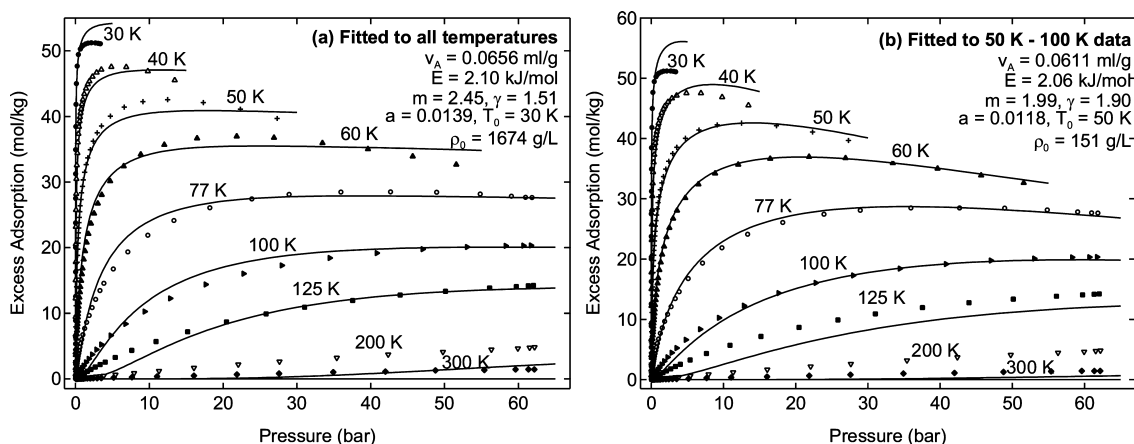
Figure 2. Fits of the D−A equation (eq 5) to benchmark MOF-5 experimental hydrogen adsorption data from ref 7. (a) Model fitted over the complete temperature range. (b) Model fitted to data between the 50 and 100 K temperature range.

While MOF-5 and AX-21 both possess similar total micropore volumes, the pore structures in AX-21 are highly heterogeneous in comparison to MOF-5, with some fraction of those pores corresponding to strong adsorption sites. This leads to a steeper H_2 isotherm shape at low pressures. Activated Cu-BTC contains coordinatively unsaturated metal center (CUMC) sites which bind H_2 by strong Coulomb interactions, also leading to a greater adsorption at low pressure. While the modified D−A model is effective in describing the H_2 adsorption isotherms exhibited by materials such as AX-21 and Cu-BTC, it may not necessarily be effective for MOF-5.

We evaluated the effectiveness of the modified D−A model (eq 4) on a set of benchmark MOF-5 hydrogen adsorption isotherms available over a wide temperature range of 30−300 K.[7] Because these measurements contain many data points at low pressure (<0.1 bar), yet fewer at high pressures, we have reweighted the data so that it is more evenly distributed across the complete range of pressure for each isotherm. We tried fitting eq 4 to the reference MOF-5 isotherms using many different criteria, such as fitting only high and low temperatures and fitting only between 77 and 300 K. One representative fit is displayed in Figure 1, while the remainder are available in Figure S1. It does not appear possible to accurately fit the entire temperature range while keeping the heterogeneity parameter fixed at $m = 2$. In particular, the model yields negative uptake values at 200 and 300 K. To fit the MOF-5 isotherm across the entire temperature range, it was necessary to set $m = 12.4$, as shown in Figure 1a. However, this results in an unrealistically large characteristic free energy, $E = 3.67 + 0.195 \times T$ (e.g., with values of 18.6 kJ/mol at 77 K and 61.2 kJ/mol at 295 K). As displayed in Figure 1b, modeled isotherms for these parameters still have negative values at 300 K up to a pressure of 27 bar. The assumptions of a temperature-independent p_s and a linear temperature variation for $E = a + bT$ cause the modified D−A model to consistently underestimate the adsorbate density at 200 and 300 K, resulting in negative excess adsorption values at low pressures. Apparently the reason this problem does not arise for AX-21 or Cu-BTC is that the adsorption isotherms for these materials are steeper than those of MOF-5 at low pressures due to their larger adsorption enthalpies.

To obtain satisfactory fits for eq 4 across the complete temperature range, while retaining reasonable values for the model parameters, it is necessary to fit p_s and E independently for each temperature. Details of these fits are provided in Figure S1 in the Supporting Information. The temperature variation of p_s is described by a power law expression, varying by 5 orders of magnitude between 30 and 300 K. It appears that E does not vary linearly with temperature as originally assumed but is described instead by a second-order polynomial, increasing from 2.4 kJ/mol at 30 K to 18.2 kJ/mol at 300 K. Regardless of how the physical significance of p_s and E is interpreted, it is clear that the modified D−A model is not a convenient tool for

modeling H_2 adsorption in MOF-5 across a wide temperature range. Since the empirical temperature variation of p_s and E is not known a priori, it requires 21 adjustable parameters to fit the 9 experimental temperatures (i.e., a unique p_s and E for each temperature).

The D−A model has been previously applied to MOF-5 hydrogen uptake over a narrow 50−87 K temperature range.[6] Instead of assuming a constant adsorbate volume, as in eq 4, the fractional volume-filling interpretation was used in which micropores are gradually filled with a liquidlike hydrogen adsorbate phases, similar in density to liquid hydrogen but with a thermal expansion factor. The adsorbate volume increases with adsorption up to a maximum value (V_a). Excess adsorption is equal to

$$n_{ex} = (\rho_a - \rho_g)V_a \exp\left[-\left(\frac{RT}{E}\ln\frac{p_s}{p}\right)^m\right] \quad (5)$$

where the adsorbate density and pseudosaturation pressure are both assumed to vary with temperature according to

$$\rho_a = \rho_0 \exp[-a(T - T_0)] \quad (6a)$$

$$p_s = p_c(T/T_c)^\gamma \quad (6b)$$

We tested the fits of the eqs 5−6 using the same set of benchmark MOF-5 isotherms. Two representative fits are shown in Figure 2. As is apparent from both panels in Figure 2, this model is only useful for describing narrow, cryogenic temperature ranges such as 50−100 K. At higher temperatures the assumption of a liquidlike hydrogen adsorbate phase is questionable. Therefore, the model greatly underpredicts the adsorbate volume at 200 and 300 K, resulting in negligible excess adsorption. In panel (a), where the model was fitted to all temperatures, the agreement between model and experimental data was poor for all temperatures. Further, fits to the entire set of isotherms yields unrealistic values for some parameters, such as a characteristic adsorbate density $\rho_0 = 1674$ g/L which is more than 20 times larger than the density of liquid hydrogen. In panel (b) of the same figure, the model was fitted only to the 50−100 K data, resulting in very poor fits outside that temperature range. To obtain satisfactory fits of eqs 5−6 across a wide temperature range, it is necessary to fit the characteristic free energy E independently for each temperature. These results are available in the Supporting Information in Figure S2. Since there is no general formula for the temperature variation of E, it requires 14 adjustable parameters to fit the 9 experimental isotherms (a unique E for each temperature). These results demonstrate that eqs 5−6 are not a significant improvement upon the modified D−A equation in eq 4 with regard to the quality of fits to hydrogen adsorption in MOF-5 across a wide temperature range.

Unilan Model. In light of the limitations of the above pore-filling models in reproducing experimental isotherms, we have investigated whether MOF-5 hydrogen adsorption isotherms may be better described by monolayer models. The motivation for this is that the MOF-5 crystalline pore structure contains comparatively large channels (7.8 Å) and pore cavities (12.1 and 15.2 Å), and lacks unscreened CUMC sites, resulting in less adsorption at low pressures. The simplest surface adsorption model is the Langmuir equation, where absolute adsorption is given by

$$n_a = \frac{n_{max}}{1 + K/p} \quad (7)$$

The equilibrium constant is given by

$$K = p°\exp\left[-\frac{\Delta S}{R} + \frac{\Delta H}{RT}\right] \quad (8)$$

where ΔH is equal to the (constant) molar differential enthalpy of adsorption and ΔS can be interpreted as the molar integral entropy at $n_a = n_{max}$.[40] The standard-state pressure is $p° = 1$ bar. The Langmuir model neglects surface heterogeneity and does not provide a realistic description of supercritical hydrogen adsorption by most microporous materials. In one study, however, a superposition of two Langmuir isotherms was successfully fitted to the reference MOF-5 isotherms over the complete temperature range.[41] For our purpose, we would like to use a model which has fewer parameters (e.g., than a superposition of two or more Langmuir isotherms) and for which there is a clearer physical interpretation of the parameter values.

Because MOF-5 lacks unscreened CUMC adsorption sites, this implies that the surface heterogeneity should be less than that found in AX-21 and Cu-BTC. This has been established by the following experimental results and first-principle calculations. Comparative hydrogen isotherm measurements showed that there is substantially less hydrogen uptake at low pressures in MOF-5 compared to materials with greater surface heterogeneity and larger adsorption enthalpies such as activated carbons, Cu-BTC, and zeolite NaX.[9,42] Inelastic neutron-scattering studies of MOF-5 have identified up to four H_2 binding sites, but note that the distribution of rotational barriers (a probe of the local chemical environment surrounding an adsorption site) is considerably less complex in MOF-5 compared to other MOFs in the study.[43] First-principles calculations at the MP2 and CCDS(T) level have recently found that the binding energy of the inorganic cluster (4.4−5.2 kJ/mol) and organic linker (5.4 kJ/mol) are actually quite close in value.[44]

The Unilan model (i.e., *uni*form energy distribution and *Lang*muir local isotherm) is an attractive empirical model for describing hydrogen adsorption in MOF-5. It uses the (monolayer) Langmuir equation to describe the local isotherms. This model treats energetic heterogeneity by assuming a uniform distribution of adsorption enthalpies between E_{max} and E_{min} and zero elsewhere.[45−49] The probability density function that an adsorption site has enthalpy q is given by

$$N(q) = \begin{cases} 1/(E_{max} - E_{min}) & \text{if } E_{min} < q < E_{max} \\ 0 & \text{elsewhere} \end{cases} \quad (9)$$

where the positive-valued q has been substituted for $-\Delta H$. Adsorption at a local patch with enthalpy q is assumed to follow the Langmuir equation. Rather than taking a discrete superposition of Langmuir equations, this model instead averages the Langmuir equation over a continuous interval from E_{min} to E_{max}. The expression for the Unilan model is obtained by evaluating the average

20203

dx.doi.org/10.1021/jp305524f | *J. Phys. Chem. C* 2012, 116, 20199−20212
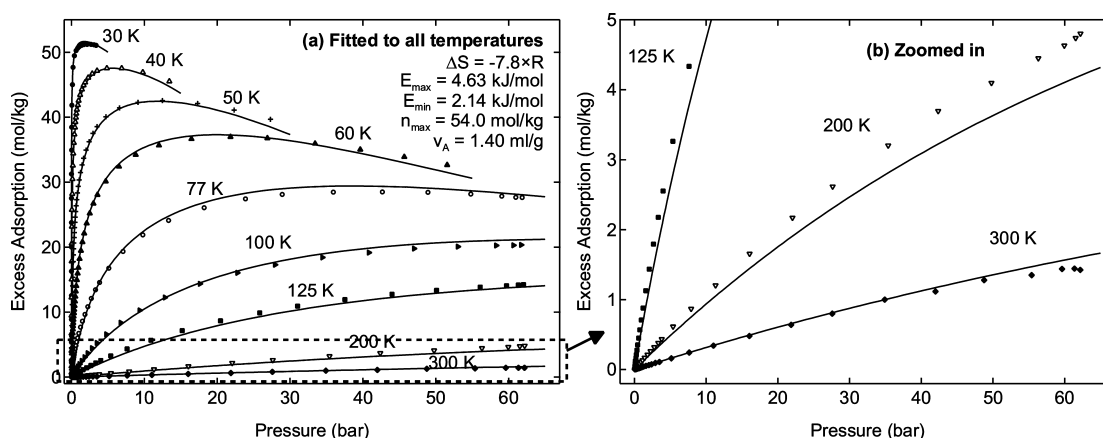
Figure 3. Fits of the Unilan equation (eq 10) to the experimental MOF-5 isotherm data points from ref 7. (a) Model fitted to all temperatures. (b) Same fits, zoomed in to the excess adsorption range of 0–5 mol/kg.

$$n_a = n_{max} \int_0^\infty \frac{N(q)}{1 + \frac{a}{p}\exp\left(-\frac{q}{RT}\right)}\,dq$$

$$= \frac{n_{max}RT}{E_{max} - E_{min}}\ln\left(\frac{a + pe^{E_{max}/RT}}{a + pe^{E_{min}/RT}}\right) \quad (10)$$

where $a = \exp(-\Delta S/R)$. The function increases monotonically versus p and meets the required properties $n_a(0) = 0$ and $n_a(\infty) = n_{max}$. It reduces to Henry's law ($n_a = k_h p$) in the low pressure limit. An implicit assumption is that the adsorption entropy is constant for all sorption sites. To calculate the excess adsorption, the standard expression $n_{ex} = n_a - \rho_g v_a$ is used. As fitted to excess adsorption data, therefore, the Unilan model contains five temperature-independent parameters: $\{\Delta S, E_{max}, E_{min}, n_{max}, v_a\}$.

A fit of the Unilan model to the reference powder MOF-5 isotherms at all temperatures is displayed in Figure 3, with additional results available in Figure S3. Whether fitted to a subset of temperatures, or to all temperatures, the quality of the Unilan model fits are superior to those of eqs 4 and 5. Furthermore, the parameters all have physically reasonable values. The entropy difference ($-7.8R$) is very close to the $-8R$ value that is typical for H_2 adsorption in many adsorbents.[49] The values of E_{max} (4.63 kJ/mol) and E_{min} (2.14 kJ/mol) are consistent with the reported experimental values of the isosteric heat (which decreases from 4.8 kJ/mol at 0 to 3.3 kJ/mol at 8 wt % excess). The estimated adsorbate volume v_a varies between 1.2 and 1.4 g/cm^3 depending on the fit criteria, a value which is slightly larger than the measured MOF-5 open-pore volume of 1.2 g/cm^3. Unlike the modified D–A models, the Unilan model accurately predicts hydrogen adsorption near room temperature (Figure 3b), with no negative values. Using only five temperature-independent parameters, each having a clear physical interpretation (e.g., no pseudosaturation pressure), the Unilan model provides an accurate and straightforward description of supercritical hydrogen adsorption across a wide temperature range. (Presumably, the fits could be improved even further by allowing either ΔS or ΔH to vary with temperature, but this appears unnecessary.) Furthermore, parameters determined from fits only to the 77, 200, and 300 K temperatures still provide accurate estimates for intermediate temperatures between those limits (see Figure S3).

Tóth Model. We also investigated fits of the reference powder MOF-5 isotherms to a frequently used empirical model, the Tóth equation, which was originally proposed for monolayer adsorption.[50] This equation has been previously found to provide good fits to hydrogen adsorption in molecular sieve carbon, zeolite NaX, Cu-BTC, and Trip(Me)-PIM at a temperature range of 77–137 K and pressure range of 0–15 bar,[42] as well as in the Cu_2(tptc) framework material over 50–100 K.[51] Fits of the Tóth equation to the reference MOF-5 data from ref 7 are available in Figure S4. The Tóth equation does not fit the 30–300 K isotherms as effectively as the Unilan model. The advantage of the Unilan model over the Tóth model may be due to its uniform energy distribution between E_{min} and E_{max}. Nonetheless, the Tóth equation still provides a significant improvement over the modified D–A equations (eqs 4 and 5–6) in terms of the quality of fits across 30–300 K, and the small number (five) of temperature-invariant parameters.

In concluding this section we note that based on the parameters in Figure 3, the maximum adsorbate density ($n_{max}/v_a = 77$ g/L) exceeds the density of liquid H_2 at the boiling point (70.8 g/L). This is based on a strict physical interpretation of v_a as the true adsorbate volume, and occurs for all the models tested here. In comparison, at the triple point (13.8 K, 0.07 bar) the density of liquid hydrogen is 77 g/L while the density of solid hydrogen is 86.5 g/L. Further, for supercritical adsorption the maximum density corresponds to a point where the adsorbate phase is incompressible, which may be between the liquid and solid hydrogen densities.

■ RESULTS

Hydrogen Storage at 77 K. Having shown that the Unilan model yields good agreement with the benchmark hydrogen adsorption data from ref 7, we now apply it to model uptake in composite materials based on mixtures of ENG and MOF-5. As described above, these materials are of interest for improving the thermal conductivity of MOF-5-based hydrogen storage systems. First, hydrogen adsorption isotherms at 77 K were measured for a complete set of ENG/MOF-5 composites (0–10% ENG) for several densities. The measured samples were

- powder MOF-5 (ρ_{bulk}: 0.13 g/cm^3)
- 0% ENG (ρ_{env}: 0.31, 0.41, 0.52, 0.60, 0.79 g/cm^3)
- 1% ENG (ρ_{env}: 0.49 g/cm^3)
- 5% ENG (ρ_{env}: 0.32, 0.47, 0.65 g/cm^3)
- 10% ENG (ρ_{env}: 0.32, 0.48, 0.72 g/cm^3)

Because the 1% ENG composites did not show significant improvement in thermal conduction properties, hydrogen isotherms were measured for only a single density.

The 77 K isotherms for all medium density (i.e., 0.5 g/cm^3) composites are shown in Figure 4. (The plotted isotherms
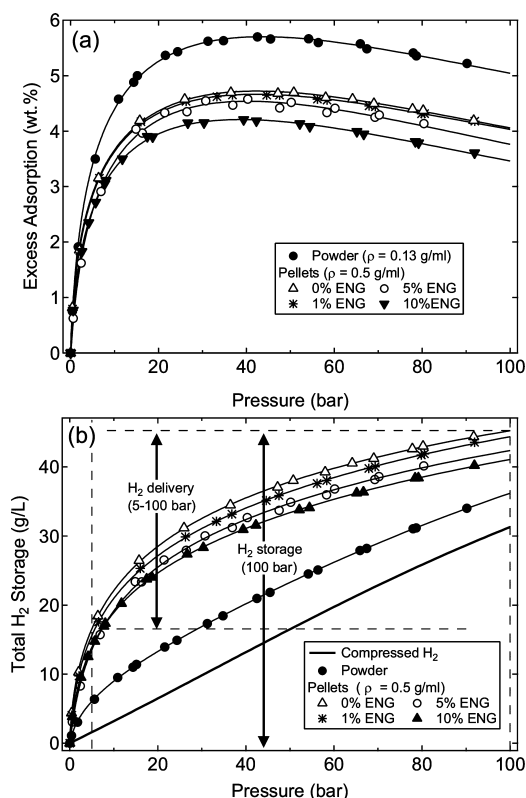
Figure 4. Hydrogen adsorption isotherms measured at 77 K for medium-density ($\rho_{env} \approx 0.5$) composite pellets. Powder MOF-5 data is included for comparison. (a) Excess adsorption isotherms, where the excess amounts are presented as a percentage of the combined hydrogen and sample mass. (b) Total volumetric hydrogen storage; cryo-compressed hydrogen is included for comparison. Hydrogen storage at 100 bar and delivery at 5 bar is illustrated for the 0% ENG data series.

include both the adsorption and desorption curves, which is why many of the data points occur in pairs.) Excess adsorption for the medium-density composites are compared with powder MOF-5 in the top panel. In the lower panel, the total volumetric storage (eq 3) is compared with the density of cryo-compressed H$_2$ at 77 K. Total hydrogen storage at 100 bar, along with hydrogen delivery at 5 bar, is illustrated for the 0% ENG data series. A compilation of the 77 K isotherms for all MOF-5/ENG composites is available in Figure S5.

Hydrogen storage at 77 K for the complete series of MOF-5/ENG composites is summarized in Figure 5, and values are listed in Table 1. In Figure 5a, maximum excess hydrogen adsorption amounts at 77 K, on a gravimetric basis in units of wt % (i.e., hydrogen mass as a percentage of combined sample and hydrogen mass), are plotted versus sample density. For all samples measured in this study the maximum in the excess adsorption occurs at a pressure between 37 and 43 bar. The figure shows a nearly linear decrease of maximum excess gravimetric adsorption versus sample density. (Because the prepared pellets used for the experiment have densities which vary slightly from the standard 0.3, 0.5, and 0.7 g/cm^3 densities

used as a basis of comparison, linear interpolation is used to estimate the values at the standard densities.) For the pellets with 0% ENG added, the 0.3 g/cm^3 pellets have no decrease compared to powder MOF-5, while the 0.5 g/cm^3 pellets have a decrease of about 17%. On a volumetric basis, however, the maximum excess increases relative to the powder by a factor of 2.6 and 3.1 at densities of 0.3 and 0.5 g/cm^3, respectively. Adding 10% ENG to neat MOF-5 pellets decreases the maximum gravimetric excess by 17%, 13%, and 6% at densities of 0.3, 0.5, and 0.7 g/cm^3, respectively. The decrease in maximum volumetric excess (for the same series of pellet densities) is approximately 22%, 12%, and 4%, respectively. As suggested by the smaller slope of the 5% and 10% ENG traces, the addition of ENG mitigates the reduction of hydrogen adsorption capacity, and surface area, at higher densities. It appears that ENG additions may protect MOF-5 crystallites from plastic deformation and/or amorphization during uniaxial compaction.[25]

In Figure 5b the maximum gravimetric excess at 77 K is plotted versus the BET specific surface area measured for each sample. Variation between the two variables roughly follows the empirical 500 m^2/g per 1 wt % rule which is observed for many framework and active carbon adsorbents.[52] While micropore volume is thought to be the more important determinant of hydrogen adsorption capacity,[53] the N$_2$ BET surface areas and micropore volumes appear to be well correlated for MOF-5/ENG composites.

The volumetric total storage (eq 3) at 100 bar and 77 K for MOF-5/ENG composites, reflecting the total mass of hydrogen inside the tank divided by the internal volume of the tank, is shown in Figure 5c. This value equals the total amount of hydrogen that can be delivered from the storage tank with starting conditions of 100 bar and 77 K, assuming that the storage media is heated to release any residual adsorbed hydrogen remaining at low pressures. The volumetric storage of cryo-compressed hydrogen at 77 K (lower line) is shown for comparison. As summarized in Figure 5c, the volumetric total storage increases with sample density for the MOF-5 composites. For 0.5 g/cm^3 density 0% ENG pellets, there is a 41% improvement compared to cryo-compressed hydrogen and 23% improvement compared to powder MOF-5. The addition of ENG produces only a small decrease for volumetric storage relative to neat MOF-5 media of equal density. For the composites with density 0.5 g/cm^3, the penalty for the addition of 10% ENG is a 6% decrease in total volumetric storage. For 0.7 g/cm^3 composites, the "weight penalty" for 10% ENG addition is only a 3% decrease in storage.

The most efficient way to pack MOF-5, without reducing micropore volume, would be as a single-crystal monolith. The theoretical hydrogen storage for a single-crystal MOF-5 monolith, occupying the entire storage tank, is drawn as the upper line in Figure 5c. We calculate this value using the maximum excess gravimetric amount, n_{ex}, from powder MOF-5 (assuming no decrease in micropore volume), but replacing $\rho_{bulk} = 0.13$ g/cm^3 with $\rho_{sc} = 0.605$ g/cm^3 in eq 2. Neat MOF-5 pellets with a density between 0.3 g/cm^3 and 0.7 achieved approximately 83% of the volumetric hydrogen storage of a MOF-5 single crystal. This is a promising development given the simplicity of uniaxial mechanical compaction and its potential for scale-up.

From a practical perspective, the most interesting quantity is the net amount of hydrogen that can be delivered to the fuel cell stack. We use 5 bar as the minimum necessary pressure for
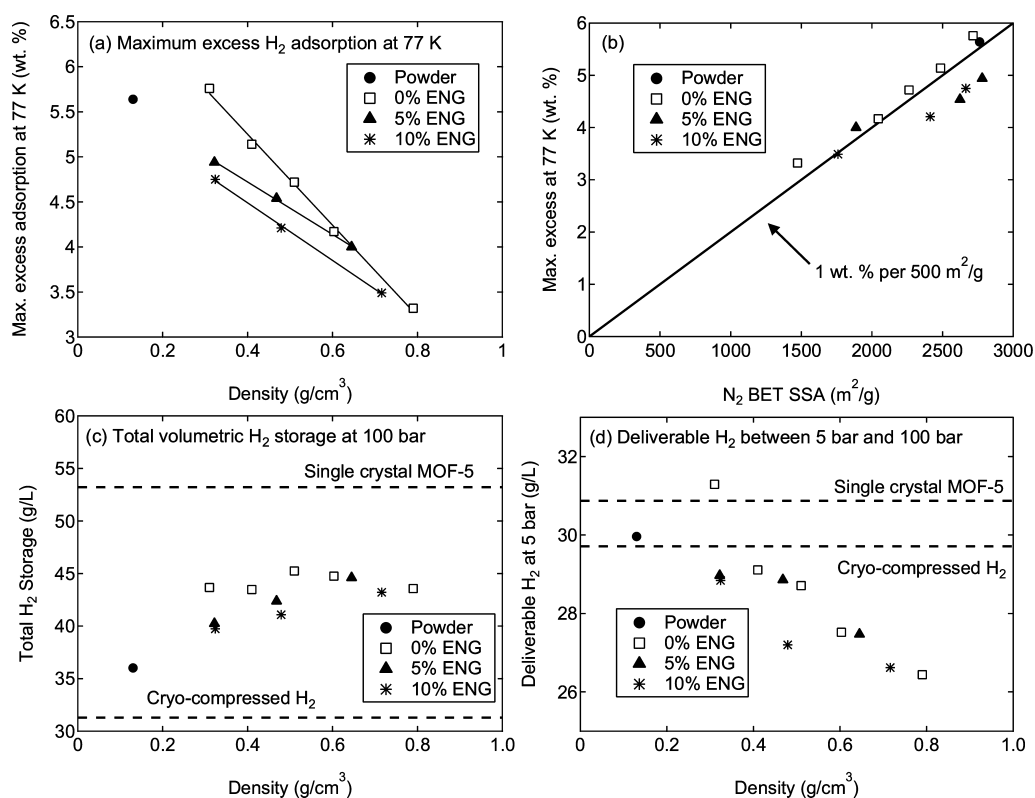
Figure 5. Summary of hydrogen storage properties at 77 K for the MOF-5/ENG composites. (a) Maximum gravimetric excess hydrogen adsorption versus sample density. (b) Maximum gravimetric excess hydrogen adsorption versus N_2 BET specific surface area. (c) Total volumetric hydrogen storage at 100 bar, compared with the values for cryo-compressed hydrogen at 77 K and the estimated upper limit for single-crystal MOF-5. (d) Total hydrogen delivery between 5 and 100 bar, compared with values for cryo-compressed hydrogen at 77 K and single-crystal MOF-5.

**Table 1. Hydrogen Adsorption Properties at 77 K of MOF-5/ENG Composites**

sample		surface area	maximum excess adsorption		deliverable H_2	
ENG %	ρ (g/cm³)	BET(N_2) (m²/g)	gravimetric (wt %)	volumetric (g/L)	100−0 bar (g/L)	100−5 bar (g/L)
0	0.31	2716	5.76	19.1	43.7	31.3
0	0.41	2486	5.14	22.2	43.5	29.1
0	0.52	2263	4.72	25.7	45.3	28.7
0	0.60	2045	4.17	26.3	44.7	27.5
0	0.79	1473	3.32	27.1	43.6	26.4
1	0.49	2584	4.66	24.1	44.4	28.8
5	0.32	2781	4.94	16.7	40.3	29.0
5	0.47	2623	4.54	22.3	42.4	28.9
5	0.65	1888	4.00	26.9	44.6	27.5
10	0.32	2665	4.75	16.1	39.7	28.8
10	0.48	2413	4.21	21.0	41.1	27.2
10	0.72	1760	3.49	25.9	43.2	26.6
powder		2762	5.64	7.8	36.0	30.0
single-crystal		2762	5.64	36.2	53.2	30.9
cryo-compressed		N/A	N/A	N/A	31.3	29.7

the fuel cell intake and 100 bar as the maximum. The isothermal hydrogen delivery amount (at T = 77 K) can be estimated as the difference in the total hydrogen storage at 100 and 5 bar. These values for the MOF-5/ENG composites are summarized in Figure 5d. Due to the uptake of hydrogen at low pressures (Figure 4b), a significant fraction of hydrogen remains adsorbed at the desorption conditions of 77 K and 5 bar; consequently, MOF-5 compacts show no improvement in deliverable hydrogen compared to cryo-compressed hydrogen. For the neat MOF-5 pellets of density 0.5 g/cm³, the isothermal hydrogen delivery is actually decreased by about

3% compared to cryo-compressed hydrogen. As described later, at temperatures above 77 K the isothermal hydrogen delivery from MOF-5/ENG composites exceeds that of cryo-compressed hydrogen. Moreover, the use of a simultaneous temperature and pressure swing — e.g., adsorption at 77 K and 100 bar, desorption at 160 K and 5 bar — results in a 44% increase (0.5 g/cm³ pellets) in usable hydrogen compared to cryo-compressed.

Variable Temperature Hydrogen Adsorption. Hydrogen isotherms were measured at intermediate temperatures (between 77 and 295 K) for composites with the most
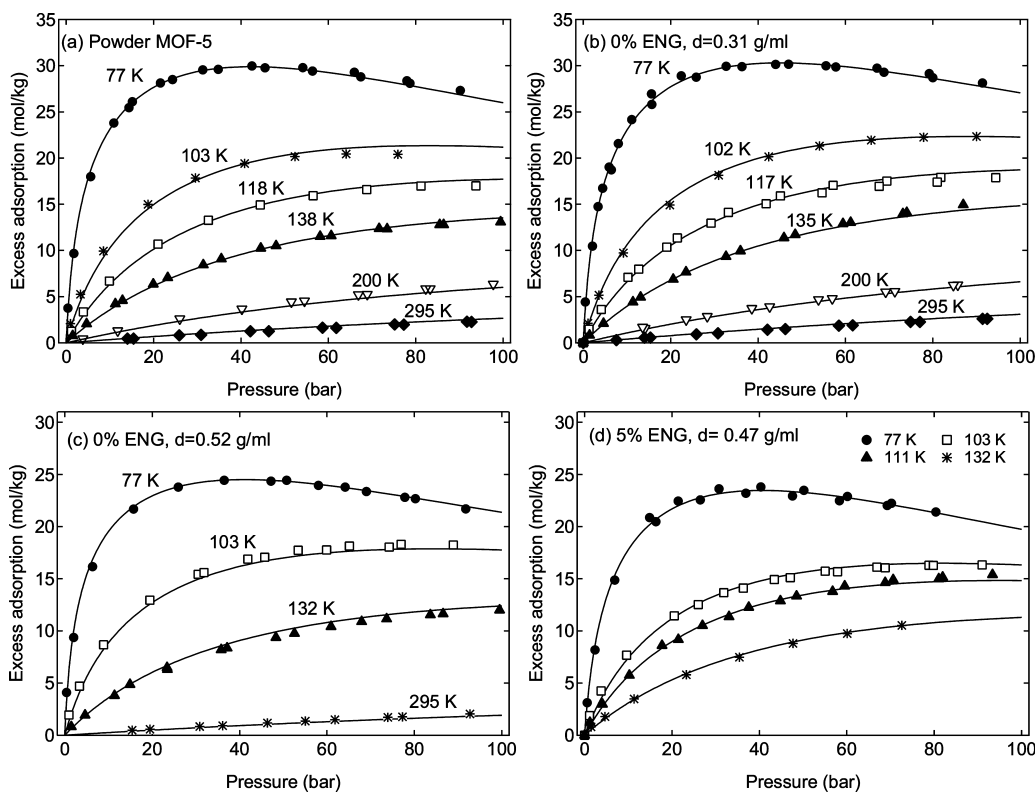
Figure 6. Measured intermediate temperature hydrogen isotherms for selected MOF-5/ENG composites, with fits to the Unilan model. (a) Powder MOF-5, (b) neat MOF-5 pellets with density ρ_{env} = 0.31 g/cm^3, (c) neat MOF-5 pellets with density ρ_{env} = 0.52 g/cm^3, and (d) 5% ENG pellets with density ρ_{env} = 0.47 g/cm^3.

Table 2. Unilan Model Parameters for H$_2$ Adsorption by Select MOF-5/ENG Composites

sample		(a) best fits					(b) constraints[a]	
ENG %	ρ (g/cm^3)	ΔS ($\times R$)	E_{max} (kJ/mol)	E_{min} (kJ/mol)	n_{max} (mol/kg)	v_a (cm^3/g)	n_{max} (mol/kg)	v_a (cm^3/g)
powder	0.13	−7.93	5.04	1.06	67.8	1.40	64.1	1.40
0	0.31	−7.89	4.98	1.31	63.3	1.28	63.3	1.28
0	0.52	−8.08	5.30	2.05	42.4	0.91	53.9	1.21
5	0.32	−7.88	5.03	2.03	44.7	1.03	55.3	1.23
5	0.47	−7.88	4.76	2.11	41.3	0.95	48.0	1.00
10	0.32	−7.87	4.95	1.93	44.7	1.04	53.0	1.19
10	0.48	−7.86	4.96	1.55	44.6	1.08	47.5	1.11

[a]Constraints: ΔS = −7.89R, E_{max} = 4.98 kJ/mol, E_{min} = 1.31 kJ/mol.

promising thermal and H$_2$ storage properties. Isotherms for the following samples are shown in Figure 6:
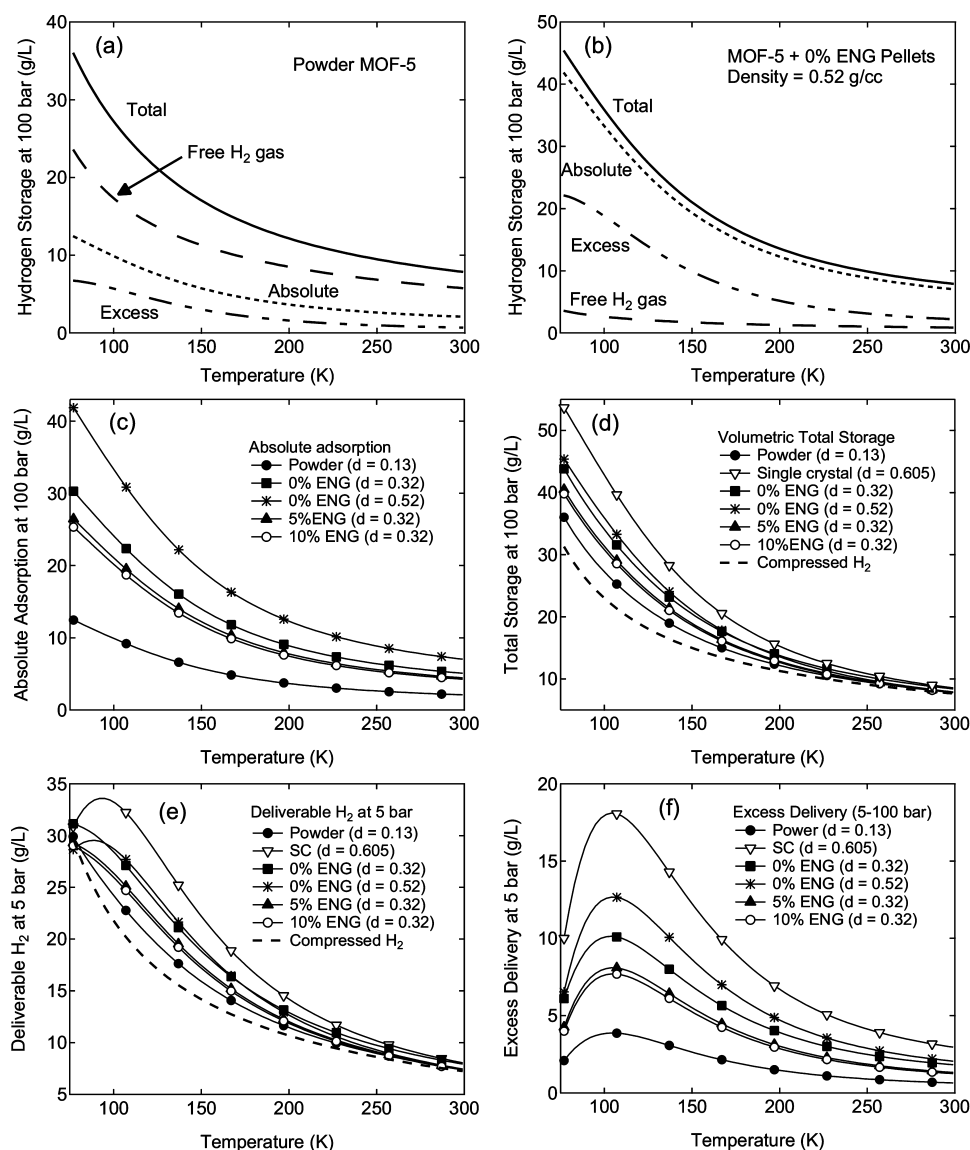
- powder MOF-5
- 0% ENG, (0.31 and 0.52 g/cm^3)
- 5% ENG (0.47 g/cm^3)

Measurements were also collected (at 77, 200, and 295 K only) for three additional samples not shown in the Figure 6:

- 5% ENG (0.32 g/cm^3)
- 10% ENG (0.32 and 0.48 g/cm^3)

We find that fitting the Unilan model to 77, 200, and 300 K hydrogen isotherms is sufficient to accurately estimate excess adsorption at intermediate temperatures and pressures. (However, the plotted curves in Figure 6 in this section were obtained by fits of the Unilan model to all available temperature series.) The Unilan model provides excellent fits to the measured isotherms across the entire temperature range.

Unilan model parameters corresponding to a minimum sum of squared residuals (SSR) between fits and data are summarized in Table 2a. In these fits, all five parameters were allowed to vary independently without any constraints until a minimum SSR was reached. Notably, the modeled isotherms based on the parameters in Table 2a for powder MOF-5 are in good agreement with the reference MOF-5 isotherms from ref 7 (shown in Figure S3d). Some trends in the Unilan model parameters for the MOF-5/ENG composites may be artifacts arising from the nonlinear fitting. In particular, there is an inverse correlation between the E_{min} and n_{max} model parameters. To find more meaningful trends in the parameters, some should be held constant during the fit. The entropy and enthalpy parameters are not expected to change significantly with density and small ENG additions. Fits were therefore performed with ΔS, E_{max}, and E_{min} held constant at the values for neat 0.31 g/cm^3 pellets, leaving n_{max} and v_a as the only adjustable parameters. The addition of these three constraints

Figure 7. Total hydrogen storage at 100 bar versus temperature for selected MOF-5/ENG composites, using Unilan model parameters from Table 2b. (a) Hydrogen storage in powder MOF-5 at 100 bar; compares the relative contributions to total hydrogen storage made by excess adsorption, absolute adsorption, and bulk H_2. (b) Hydrogen storage at 100 bar in neat MOF-5 pellets with density 0.52 g/cm³. (c) Absolute hydrogen adsorption at 100 bar, on a volumetric basis, for MOF-5/ENG composites. (d) Total hydrogen storage at 100 bar (eq 3) plotted versus temperature. (e) Total hydrogen delivery between 100 and 5 bar. (f) Excess hydrogen delivery, defined here as the difference in excess adsorption, between 100 and 5 bar.

does not significantly decrease the quality of the fits (shown in Figure S6). As summarized in Table 2b, the two fitted parameters n_{max} and v_a decrease versus ENG% and density. This is consistent with our findings that micropore volume decreases with compaction and decreases to a lesser degree with ENG addition.

Hydrogen Delivery. Hydrogen storage at 100 bar for selected MOF-5/ENG composites is plotted versus temperature (77−295 K) in Figure 7 using the Unilan model parameters from Table 2b. Panel (a) breaks down the relative contributions to total hydrogen storage at 100 bar made by excess adsorption, absolute adsorption, and free H_2 in the volume $v_g = v_v − v_a$ (which can be interpreted as the interstitial volume occupied by bulk H_2 gas outside of the MOF-5 pores). The sum of the absolute adsorption and free hydrogen equals the total storage. In Figure 7b the same comparison is made for the 0% ENG pellets of density 0.52 g/cm³. This illustrates that

for a loosely packed powder, a majority of stored hydrogen simply consists of bulk hydrogen gas outside of the adsorbate volume. In contrast, for the compacted MOF-5 absolute adsorption makes up a much larger percentage of the total hydrogen storage. Only a small fraction of the stored hydrogen consists of bulk gas in the interstitial volume.

Figure 7c illustrates the volumetric absolute adsorption (n_a) at 100 bar for MOF-5/ENG composites plotted as a function of temperature. Compacting powder MOF-5 to a density of 0.52 g/cm³ increases the absolute adsorption by a factor of approximately 3. Total volumetric hydrogen storage at 100 bar is plotted versus temperature in Figure 7d. Values for single-crystal MOF-5 are extrapolated from the powder MOF-5 values by replacing $\rho_{bulk} = 0.13$ g/cm³ with $\rho_{sc} = 0.605$ g/cm³. The single-crystal MOF-5 values represent an upper limit for volumetric hydrogen storage of compacted MOF-5. Among the samples measured, volumetric storage is highest for the 0%
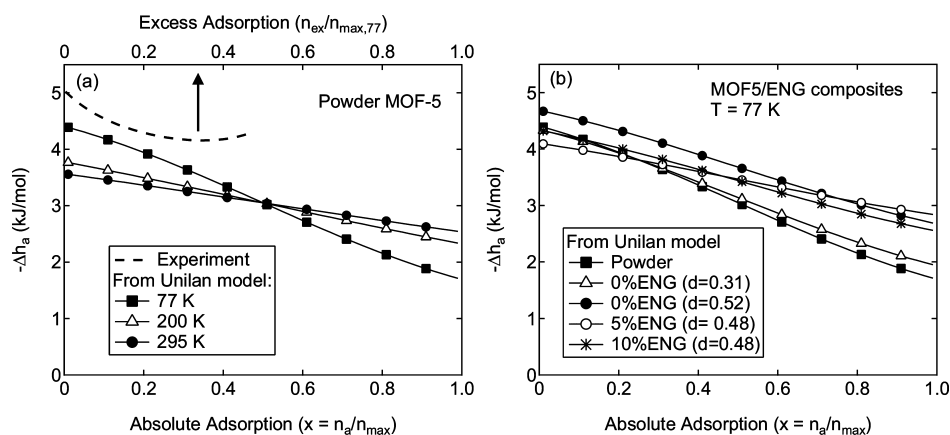
Figure 8. (a) Absolute differential enthalpy (eq 11) of powder MOF-5 at three temperatures, compared with the excess differential enthalpy estimated by direct interpolation of experimental 77, 103, and 118 K isotherms. (b) Absolute differential enthalpy (eq 11) for selected MOF-5/ENG composites, based on Unilan model parameters listed in Table 2a.

ENG pellets of density 0.52 g/cm^3. Relative to powder MOF-5 and compressed H$_2$, the largest enhancement in volumetric H$_2$ storage by MOF-5/ENG pellets occurs at temperatures close to 100 K. Neat MOF-5 pellets with density 0.52 g/cm^3 have a total volumetric storage of 36 g/L at 100 K, which is roughly 33% and 58% larger than the respective values for powder MOF-5 and compressed H$_2$. The addition of 5% and 10% ENG to the ~0.5 MOF-5 g/cm^3 pellets decreases the total volumetric storage at 100 K by about 6% and 11%, respectively.

Total hydrogen delivery (isothermal) between 100 and 5 bar is plotted as a function of temperature in Figure 7e.[54] Cryo-compressed has more deliverable hydrogen at 77 K than most MOF-5/ENG composites (with the exception of 0% ENG 0.5 g/cm^3 pellets and single-crystal MOF-5). However, above 77 K the MOF-5/ENG composites exceed cryo-compressed hydrogen in terms of deliverable hydrogen capacity. The largest improvement in isotherm delivery (relative to powder MOF-5 and compressed H$_2$) occurs at a temperature of approximately 122 K. The 0.52 g/cm^3 pellets with 0% ENG have an isothermal delivery at 122 K of 24.7 g/L, about 23% and 41% greater than the respective values for powder MOF-5 and compressed H$_2$. Addition of 5% and 10% ENG to the ~0.5 g/cm^3 MOF-5 pellets reduces the total isothermal H$_2$ delivery by about 5% and 9%, respectively.

In Figure 7e, the isothermal total delivery for compressed H$_2$ decreases monotonically versus temperature. Similarly, the low-density MOF-5 composites (~0.3 g/cm^3) also exhibit a monotonic decrease in deliverable hydrogen. On the other hand, the plotted curves for total isothermal delivery from single-crystal MOF-5 and neat 0.52 g/cm^3 pellets reach a maximum at approximately 105 K. This maximum can be traced to the behavior of the deliverable excess hydrogen (isothermal) shown in Figure 7f. Defined here as the difference in excess adsorption between 100 and 5 bar, the excess hydrogen delivery has a maximum at 105 K for all of the MOF-5/ENG composites shown in the plot. For single-crystal MOF-5 (and for MOF-5/ENG composites with densities of ~0.5 g/cm^3), the excess adsorption is relatively large compared to the amount of bulk hydrogen gas stored in the volume v_v, and this maximum in excess delivery curve carries over to the total storage.

Thermodynamics. The differential adsorption enthalpy, or isosteric heat, is an important quantity in adsorption studies. While the excess differential enthalpy is difficult to derive in an

analytical form for the Unilan model, the absolute adsorption enthalpy is readily calculated. After eq 10 is solved in terms of pressure, the adsorption enthalpy is calculated by the Clausius–Clapeyron equation

$$-\Delta \bar{h}_a = RT^2 \left(\frac{\partial \ln p}{\partial T} \right)_x$$

$$= E_{max} - \frac{(1-x)s}{1 - \exp\left[\frac{(1-x)s}{RT}\right]} - \frac{xs}{1 - \exp\left[\frac{-xs}{RT}\right]}$$

(11)

where $s = E_{max} - E_{min}$ and $x = n/n_{max}$. Values of $-\Delta \bar{h}_a$ for powder MOF-5, using the parameters from Table 2a, are plotted in Figure 8a for temperatures of 77, 200, and 295 K. The value at $x = 0.5$ is equal to $(E_{max} + E_{min})/2$ for all temperatures. The differential enthalpy for the Unilan model approaches a finite value as x approaches zero coverage.

Figure 8a compares the experimental $-\Delta \bar{h}_{ex}$ values determined by direct interpolation of powder MOF-5 experimental excess data with the theoretical values derived from the Unilan model. Estimating differential excess enthalpies by the isosteric method is highly sensitive to both the interpolation method[42] and the temperature and pressure ranges of the measurement.[55] We measured separate low-pressure isotherms (<3 bar) at 77 K, not shown in Figure 6a, using a high-resolution pressure transducer to improve accuracy. The interpolation method consisted of fitting rational functions to p vs n_{ex} data independently for each temperature. Temperatures included in the isosteres were 77, 103, and 118 K. Further details on the calculation of the experimental differential enthalpy are provided in Figure S7 in the Supporting Information.

The experimental $-\Delta \bar{h}_{ex}$ shown in Figure 8a as the dashed line is plotted as a function of fractional excess adsorption $n_{ex}/n_{m,77}$, where $n_{m,77}$ is the maximum excess adsorption at 77 K. Above $n_{ex}/n_{m,77} = 0.35$ the enthalpy actually starts to increase, an effect that arises from the maximum which is present in the excess adsorption curve.[56] The experimental $-\Delta \bar{h}_{ex}$ for powder MOF-5 is slightly larger than the modeled $-\Delta \bar{h}_a$ obtained from the best-fit Unilan parameters. Figure 8b displays the modeled differential enthalpy for selected MOF-5/ENG composites using the best-fit Unilan parameters from Table 2a. As discussed earlier, these model Unilan parameters may exhibit

artifacts from the fitting process. On the other hand, since eq 11 depends only on E_{min}, E_{max}, and T, the constrained Unilan parameters from Table 2b simply yield identical enthalpies. The Clausius−Clapeyron expression in eq 11 assumes the following: (1) the adsorbate molar volume is negligibly small compared to that of the gas phase; (2) the gas phase equation of state is described by the ideal gas law. In Figure 8a, the differential enthalpies at 200 and 300 K, at low fractional coverage, are the cases that best adhere to these assumptions. Therefore, they may represent that best estimate of $-\Delta \bar{h}_a$.

■ DISCUSSION

A primary aim of this study was to explore the effects of pellet density and ENG addition on the hydrogen storage properties of MOF-5 composites. The improved thermal properties of the MOF-5/ENG composites at room temperature have been previously established, with a factor of 3 increase for 5% ENG and a factor of 5 increase for 10% ENG.[25] Although ENG has a similar skeletal density as MOF-5, it has a low surface area; therefore, ENG addition is expected to lower the hydrogen storage capacity relative to neat MOF-5 pellets by the addition of extra mass to the pellet. For a 10% ENG composite, for example, we would expect the excess hydrogen adsorption amounts (gravimetric and volumetric) to be roughly 10% lower compared to neat MOF-5 pellet of equal density. There would be a smaller reduction in total hydrogen storage, as this amount also includes the bulk gas hydrogen contained in the void volume ν_v. However, as previously described,[25] the ENG may protect MOF-5 crystallites from plastic deformation during uniaxial compression, thereby enhancing the hydrogen storage density in higher density pellets. Our results, as summarized in Figure 5, indicate that ENG additions do decrease the maximum excess adsorption at 77 K but that these additions also mitigate the loss of hydrogen storage capacity at high pellet densities. The best compromise between improved thermal conduction, increased volumetric H_2 storage density, and a reduced penalty on gravimetric excess adsorption appears to be at an ENG addition of 5−10 wt % and a pellet density close to 0.5 g/cm^3. Optimal ENG and compaction values must also be determined on a system level to balance effects such as mass transport and heat exchanger efficiency.

An unanticipated finding from this work was the effectiveness of the Unilan model, in comparison to the modified D−A model, in describing hydrogen adsorption in MOF-5 and MOF-5/ENG composites across a wide temperature range. The Unilan model accomplishes this while using only five temperature-invariant parameters, each with a plausible physical interpretation. In contrast, the modified D−A model requires at least two temperature-dependent parameters (out of five or six in total) in order to achieve fits of similar quality. There are several reasons why MOF-5 would be well described by a monolayer-based adsorption model, and by the Unilan model in particular. First, hydrogen adsorption at supercritical temperatures in large pores may tend toward monolayer formation due to the weak intermolecular interactions. The D−A model has particular difficulty in fitting MOF-5 hydrogen isotherms at higher temperatures such as 200 and 300 K, where the application of a model derived for pore filling by a liquidlike hydrogen phase is questionable. Second, hydrogen uptake in the large pores of MOF-5 has a small, and relatively homogeneous, differential adsorption enthalpy, resulting in reduced uptake at low pressures. In contrast, the modified D−A models appear to be more effective for adsorbents with a larger

enthalpies and greater surface heterogeneity, such as activated carbons (i.e., complex pore structures and graphitic edge terminations) and possibly a small number of framework structures with unscreened CUMC sites (e.g., Cu-BTC, MOF-74), as these materials have a steeper isotherm shape at low pressures. While our results suggest that the Unilan model may be less suitable for heterogeneous adsorbents, further analysis on these systems is warranted. On the other hand, the Unilan model is expected to work well for hydrogen adsorption in other framework materials with large pore sizes and no unscreened CUMC adsorption sites (e.g., MOF-177, MIL-101). Validating the Unilan model for MOF-5 over wider pressure ranges, and for supercritical adsorption by gases other than hydrogen, are topics for additional work.

■ CONCLUSION

We have studied the hydrogen storage behavior of high-density MOF-5 composites containing expanded natural graphite (ENG). The addition of 5 and 10 wt % ENG to 0.5 g/cm^3 pellets had previously been found to enhance thermal conduction at 295 K by a factor of 3 and 5, respectively, relative to neat MOF-5 compacts. We compared the quality of fits of the Unilan model, Tóth model, and Dubinin−Astakhov model for hydrogen adsorption in MOF-5 and MOF-5/ENG composites over a wide temperature and pressure range. The key findings of this study are as follows:

1. The (monolayer) Unilan model provided the most accurate description of hydrogen adsorption by MOF-5 and MOF-5/ENG composites for both published data (30−300 K, 0−60 bar) and our own experimental measurements (77−295 K, 0−100 bar). Typically associated with monolayer adsorption, the Unilan model accurately fitted the complete 30−300 K temperature range using only 5 temperature-invariant parameters. To achieve fits of similar quality, the (pore-filling) D−A model requires at least two parameters (out of five or six total) to vary with temperature. This result suggests that monolayer adsorption is more applicable than pore-filling for describing supercritical H_2 adsorption in the large pores of MOF-5.

2. The total volumetric hydrogen storage density (77 K, 100 bar) for MOF-5 + 0% ENG pellets with density 0.5 g/cm^3 is approximately 23% larger than that of powder MOF-5 and 41% larger than that of cryo-compressed hydrogen. The addition of 10% ENG to the 0.5 g/cm^3 MOF-5 pellets produces a small decrease (6%) in the total volumetric hydrogen storage at 77 K compared to neat MOF-5 pellets of equal density.

3. Isothermal hydrogen delivery (volumetric) between 100 and 5 bar is larger for MOF-5/ENG composites than for powder MOF-5 and compressed H_2 at temperatures above 77 K. The largest enhancement in isothermal delivery (relative to powder MOF-5 and compressed hydrogen) for the MOF-5/ENG composites occurs at approximately 122 K. Neat MOF-5 pellets with density 0.52 g/cm^3 have an isothermal H_2 delivery of 24.7 g/L at 122 K, which is 23% and 41% greater than the respective values for powder MOF-5 and compressed H_2. Additions of 5 and 10 wt % ENG to neat MOF-5 pellets with density ~0.5 g/cm^3 reduce the delivery by about 5% and 9%, respectively.

At 122 K, a MOF-5/ENG composite with density of 0.48 g/cm^3 and 10 wt % ENG yields a total hydrogen isothermal delivery between 100 and 5 bar of 22.5 g/L. This is an increase of about 13% compared to powder MOF-5 powder and an increase of 28% compared to cyro-compressed H$_2$. Based on the combined impact of ENG addition and pellet density on thermal conductivity and hydrogen storage capacity of MOF-5 media, optimal properties are obtained for ENG additions of 5−10 wt % and pellet densities near 0.5 g/cm^3.

■ ASSOCIATED CONTENT

Ⓢ Supporting Information

Complete results for the fits of the Unilan, Tóth, and Dubinin−Astakhov models to experimental MOF-5 hydrogen isotherms; details on the calculation of the excess differential enthalpy; complete 77 K isotherms for all MOF-5/ENG composites. This material is available free of charge via the Internet at http://pubs.acs.org.

■ AUTHOR INFORMATION

Corresponding Author

*E-mail: jjpurewal@hrl.com. E-mail: djsiege@umich.edu.

Present Addresses

§Shanghai Nuclear Engineering Research & Design Institute, 29 Hongcao Road, Shanghai 20023, China.

∥AFCC Automotive Fuel Cell Cooperation Corp., 9000 Glenlyon Parkway, Burbaby, BC, Canada.

#HRL Laboratories, LLC, Malibu, CA 90265, United States.

Notes

The authors declare no competing financial interest.

■ ACKNOWLEDGMENTS

■ REFERENCES

(1) Yang, J.; Sudik, A.; Wolverton, C.; Siegel, D. J. Chem. Soc. Rev. 2010, 39, 656−675.

(2) Li, H.; Eddaoudi, M.; O'Keeffe, M.; Yaghi, O. M. Nature 1999, 402, 276−279.

(3) Dailly, A.; Vajo, J. J.; Ahn, C. C. J. Phys. Chem. B 2006, 110, 1099−1101.

(4) Wong-Foy, A.; Matzger, A.; Yaghi, O. J. Am. Chem. Soc. 2006, 128, 3494−3495.

(5) Panella, B.; Hirscher, M.; Putter, H.; Muller, U. Adv. Funct. Mater. 2006, 16, 520−524.

(6) Poirier, E.; Dailly, A. J. Phys. Chem. C 2008, 112, 13047−13052.

(7) Zhou, W.; Wu, H.; Hartman, M. R.; Yildirim, T. J. Phys. Chem. C 2007, 111, 16131−16137.

(8) Kaye, S.; Dailly, A.; Yaghi, O.; Long, J. J. Am. Chem. Soc. 2007, 129, 14176−14177.

(9) Schmitz, B.; Muller, U.; Trukhan, N.; Schubert, M.; Ferey, G.; Hirscher, M. ChemPhysChem 2008, 9, 2181−2184.

(10) Kaye, S.; Long, J. J. Am. Chem. Soc. 2005, 127, 6506−6507.

(11) Müller, U.; Schubert, M.; Teich, F.; Puetter, H.; Schierle-Arndt, K.; Pastre, J. J. Mater. Chem. 2006, 16, 626−636.

(12) Czaja, A. U.; Trukhan, N.; Müller, U. Chem. Soc. Rev. 2009, 38, 1284−1293.

(13) Jorgensen, S. W. Curr. Opin. Solid State Mater. Sci. 2011, 15, 39−43.

(14) Purewal, J. J.; Liu, D.; Yang, J.; Sudik, A.; Siegel, D.; Maurer, S.; Mueller, U. Int. J. Hydrogen Energy 2012, 37, 2723−2727.

(15) Hu, Y. H.; Zhang, L. Phys. Rev. B 2010, 81, 174103.

(16) Zacharia, R.; Cossement, D.; Lafi, L.; Chahine, R. J. Mater. Chem. 2010, 20, 2145−2151.

(17) Dailly, A.; Poirier, E. Energy Environ. Sci. 2011, 4, 3527−3534.

(18) Jordá-Beneyto, M.; Lozano-Castelló, D.; Suárez-García, F.; Cazorla-Amorós, D.; Linares-Solano, A. Microporous Mesoporous Mater. 2008, 112, 235−242.

(19) Zhang, J. S.; Fisher, T. S.; Ramachandran, P. V.; Gore, J. P.; Mudawar, I. J. Heat Transfer 2005, 127, 1391−1399.

(20) Aleksić, P.; Næss, E. ASME Conf. Proc. 2009, IMECE2009−10593, 603−610.

(21) Lamari, M.; Aoufi, A.; Malbrunot, P. AlChE J. 2000, 46, 632−646.

(22) Richard, M.-A.; Cossement, D.; Chandonia, P.-A.; Chahine, R.; Mori, D.; Hirose, K. AIChE J. 2009, 55, 2985−2996.

(23) Hirose, K.; Mori, D.; Chahine, R. J. Chem. Eng. Jpn. 2011, 44, 636−642.

(24) Huang, B. L.; Ni, Z.; Millward, A.; McGaughey, A. J. H.; Uher, C.; Kaviany, M.; Yaghi, O. Int. J. Heat Mass Transfer 2007, 50, 405−411.

(25) Liu, D.; Purewal, J. J.; Yang, J.; Sudik, A.; Maurer, S.; Mueller, U.; Ni, J.; Siegel, D. J. Int. J. Hydrogen Energy 2012, 37, 6109−6117.

(26) Kim, K. J.; Montoya, B.; Razani, A.; Lee, K. H. Int. J. Hydrogen Energy 2001, 26, 609−613.

(27) Sanchez, A. R.; Klein, H. P.; Groll, M. Int. J. Hydrogen Energy 2003, 28, 515−527.

(28) Pohlmann, C.; Rontzsch, L.; Kalinichenka, S.; Hutsch, T.; Kieback, B. Int. J. Hydrogen Energy 2010, 35, 12829−12836.

(29) Broom, D. P. Hydrogen Storage Materials; Green Energy and Technology Springer: London, U.K., 2011.

(30) Leachman, J. W.; Jacobsen, R. T.; Penoncello, S. G.; Lemmon, E. W. J. Phys. Chem. Ref. Data 2009, 38, 28.

(31) Lemmon, E. W.; Huber, M. L.; McLinden, M. O. NIST Standard Reference Database 23: Reference Fluid Thermodynamic and Transport Properties-REFPROP, Version 9.0, 2010.

(32) Lowell, S.; Shields, J. E.; Thomas, M. A.; Thommes, M. Characterization of Porous Solids and Powders: Surface Area, Pore Size, and Density; Klewer Academic: Dordrecht, The Netherlands, 2004.

(33) McGeary, R. K. J. Am. Ceram. Soc. 1961, 44, 513−522.

(34) When the storage tank mass is not included in the mass percentage, the gravimetric storage is (exceedingly) large for low-density adsorbents. That is, when ρ_{env} is small, the amount of free hydrogen within the tank ($v_v \times \rho_g$) will be very large in comparison to the sorbent mass ($m_{sorbent}$). To obtain a useful quantitative measure of gravimetric storage, the mass of the storage tank should be included. This discussion is better left for a true "system" type technical analysis, which incorporates the masses of the storage tank, insulation, heat exchangers, and other auxiliary components.

(35) Dubinin, M.; Astakhov, V. Adv. Chem. Ser. 1971, 102, 69−85.

(36) Zhou, Y. P.; Zhou, L. Sci. China, Ser. B: Chem. 1996, 39, 598−607.

(37) Richard, M. A.; Benard, P.; Chahine, R. Adsorption 2009, 15, 43−51.

(38) Stéphanie-Victoire, F.; Goulay, A.; de Lara, E. Langmuir 1998, 14, 7255−7259.

(39) Ruthven, D. M. Principles of Adsorption and Adsorption Processes; John Wiley & Sons: New York, 1984.

(40) Myers, A. L. AIChE J. 2002, 48, 145−160.

(41) Mertens, F. Surf. Sci. 2009, 603, 1979−1984.

(42) Tedds, S.; Walton, A.; Broom, D. P.; Book, D. Faraday Discuss. 2011, 151, 75−94.

(43) Rowsell, J. L. C.; Eckert, J.; Yaghi, O. M. J. Am. Chem. Soc. 2005, 127, 14904−14910.

(44) Lee, J. S. Bull. Korean Chem. Soc. 2011, 32, 4199−4204.

(45) Halsey, G.; Taylor, H. S. J. Chem. Phys. 1947, 15, 624−630.

(46) Temkin, M.; Pyzhev, V. Acta Physiochim. URSS 1940, 12, 327−356.

(47) Sips, R. *J. Chem. Phys.* **1948**, *16*, 490−495.

(48) Honig, J. M.; Reyerson, L. H. *J. Phys. Chem.* **1952**, *56*, 140−144.

(49) Bhatia, S. K.; Myers, A. L. *Langmuir* **2006**, *22*, 1688−1700.

(50) Tóth, J. *Acta Chim. Acad. Sci. Hung.* **1971**, *69*, 311−328.

(51) Bimbo, N.; Ting, V. P.; Hruzewicz-Kolodziejczyk, A.; Mays, T. J. *Faraday Discuss.* **2011**, *151*, 59−74.

(52) Chahine, R.; Benard, P. *Adv. Cryog. Eng.* **1998**, *43*, 1257−1264.

(53) Texier-Mandoki, N.; Dentzer, J.; Piquero, T.; Saadallah, S.; David, P.; Vix-Guterl, C. *Carbon* **2004**, *42*, 2744−2747.

(54) While only isothermal conditions are considered here, the amounts of deliverable hydrogen could be further increased by employing a temperature swing; i.e., upon reaching a discharge pressure of 5 bar, additional hydrogen could be extracted by heating this system.

(55) Rouquerol, F.; Rouquerol, J.; Sing, K. *Adsorption by Powders and Porous Solids*; Academic Press: London, U.K., 1999.

(56) Myers, A. L.; Monson, P. A. *Langmuir* **2002**, *18*, 10261−10273.

20212

dx.doi.org/10.1021/jp305524f | *J. Phys. Chem. C* 2012, 116, 20199−20212